

# Study of Anomalous Small-Angle X-ray Scattering near Sulfur *K*-edge

硫黄 *K* 吸収端における異常小角 X 線散乱法の研究

Department of Advanced Materials Science, 47-096039, Masashi Handa  
Supervisor: Professor Yoshiyuki Amemiya

*Keywords:* SAXS, ASAXS, absorption edge, soft X-ray, rubber

## 1 Introduction

Small-angle X-ray Scattering (SAXS) is effective in analyzing the structure of soft matter. In SAXS experiments, the scattering power of a material is usually determined by atomic scattering factor,  $f_0$ , of each element. When the energy of the incident X-ray is near the absorption edge of a specific element, its atomic scattering factor becomes complex number as

$$f(E) = f_0 + f'(E) + if''(E).$$

This relationship is called anomalous dispersion, and SAXS experiment with this relationship is called anomalous SAXS (ASAXS). Although ASAXS has been widely applied to the systems containing high-Z elements, the application to the system composed of only low-Z elements such as phosphorus, sulfur and chlorine has been restricted. The main reason of this restriction is the X-ray energy. These elements have their *K*-edges in considerably low energy region (2000 - 4000 eV). For example, the *K*-edge of sulfur is 2472 eV. It is hard to approach this energy region because there are few beamlines which provide X-rays of this energy region. In addition, SAXS experiments in this energy region require some challenges (vacuum condition, optimization of detectors for soft X-ray, monitoring of the direct beam intensity etc.). The importance of SAXS in this energy region, however, greatly outweighs these challenges because low-Z elements (phosphorus, sulfur and chlorine) play key roles in the structure of biological and synthetic polymer.

The goals of this research are (i) accurate SAXS measurements in 2000 - 4000 eV and (ii) an application of ASAXS to rubber, which leads to the elucidation of inhomogeneities of crosslinking structure in rubber.

## 2 Accurate SAXS measurement near sulfur *K*-edge

A new experimental station was developed at B-branch of BL27SU, SPring-8 (Hyogo, Japan) [2]. We surveyed several types of settings for SAXS measurement, and finally determined the arrangement as shown in Fig. 1. Main features of this arrangement are a collimating system of Kratky camera and the use of the photodiode (AXUVPSV, International Radiation Detectors Inc.). The Kratky camera was composed of two slits (S2, S3) and the photodiode, which efficiently blocks parasitic scatterings. The photodiode placed just upstream of an area detector enables us to measure the intensity of a transmitted X-ray beam during a SAXS measurement.

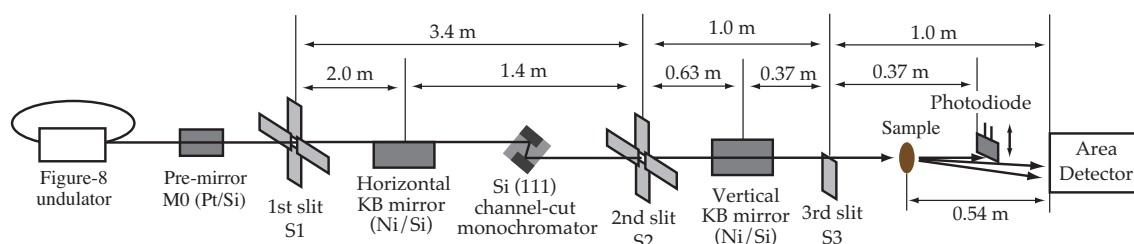


Figure 1: The new experimental setting which was built at B-branch of BL27SU.

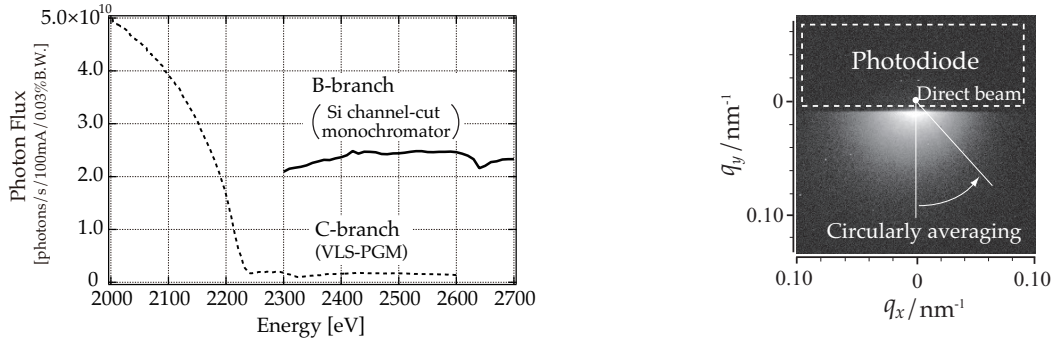


Figure 2: (Left) Photon flux obtained with the two different settings. (Right) Scattering pattern measured at E=2300 eV. Exposure time was 10 minutes.

An indirectly illuminated X-ray area detector was set for SAXS measurement. This area detector was composed of a phosphor screen (P43, Gd<sub>2</sub>O<sub>2</sub>S:Tb), an optical relay lens, and a full-frame back-illuminated CCD detector (C4742-98-KAG, Hamamatsu Photonics Co. Ltd.). B-branch has realized a high flux of 10<sup>10</sup> photons/s/100mA/0.03%B.W. (Fig. 2 left, solid line) with Si channel-cut monochromator, which is favorably compared to the flux of C-branch (dotted line) [3]. This flux was measured by using the photodiode under the condition that the sample and all slits were removed. Energy resolution,  $\Delta E/E$ , of B-branch was calculated to be  $1.3 \times 10^{-4}$ , which is approximately three times higher than that of C-branch ( $3.3 \times 10^{-4}$ ) [4] [5]. We have two options in terms of distance between the sample and the area detector (34 cm and 54 cm) in this arrangement. This leads to a wide measurable  $q$ -range of  $0.005 - 0.5 \text{ nm}^{-1}$  ( $1000 - 10 \text{ nm}$  in real space), where  $q = 4\pi \sin \theta / \lambda$  is the magnitude of the scattering vector, and  $\lambda$ ,  $2\theta$  are the wavelength of X-rays and scattering angle, respectively. In this experimental station, SAXS patterns were successfully measured at several energies in 2300 - 2500 eV, and an example is shown in Fig. 2 (right).

### 3 Application to sulfur-rich rubbers

#### 3.1 Materials

Two types of sulfur-rich rubbers were prepared as follows: an accelerator and sulfur were added to SBR according to the recipes of Tab. 1. The mixtures were crosslinked by compression molding at 170 °C for 30 minutes. They were then sliced into a piece of 30  $\mu\text{m}$  in thickness at -30 °C by using a microtome (CM3050S, Leica Microsystems Co. Ltd.).

Table 1: Recipes for samples<sup>a)</sup>

	SBR <sup>b)</sup>	Sulfur	Accelerator <sup>c)</sup>
Sample A	100	5	3
Sample B	100	20	3

a) Parts per one hundred rubber by weight.

b) Styrene Butadiene Rubber (SBR1502, JSR Corp.)

c) Noccellar CZ-G (Ouchi Shinko Chemical Industrial Co., Ltd.)

#### 3.2 Results and discussion

SAXS measurements were performed at five energies below the  $K$ -edge of sulfur (2472 eV). Exposure times were all 10 minutes. From the measured scattering patterns, we obtained scattering intensity profiles by circularly averaging the intensities of corresponding pixels (Fig. 2, right). The result of sample B is shown in Fig. 3. These profiles have already been normalized in terms of the incident X-ray intensity, the thickness of the sample, the solid angle of each pixel and the absorption by the sample. Although five profiles seems to be similar with each other as a whole, small differences of these profiles reflect the internal structure of sample B. In low- $q$  range, which is enlarged in the left of Fig. 3, the intensity profiles of (2300 - 2453 eV) decreases toward the profile of 2453 eV. After that, the profiles gradually increase toward the profile of 2469.5 eV. In general, SAXS intensity is determined by the square of the contrast of scattering length density between two phases. Then, this change in low- $q$  range is explained as follows: the scattering length density of sulfur-containing phase (I) gradually decreases as the X-ray energy approaches the edge, which leads to the decrease (2300 - 2453 eV) and increase (2465 - 2469.5 eV) of intensity profiles (Fig. 4).

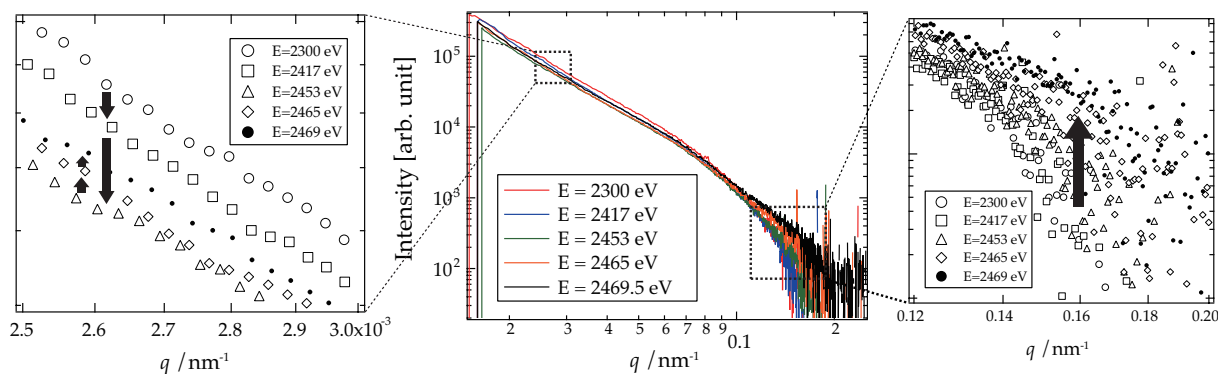


Figure 3: Scattering profiles of sample B. The  $K$ -edge of sulfur is 2472 eV, and the measurements were performed at five energies below the edge ( $E = 2300, 2417, 2453, 2465$  and  $2469.5$  eV).

In high- $q$  range ( $0.1 \text{ nm}^{-1} < q$ ) of these profiles, a gradual change is observed. This range in reciprocal space corresponds to the range of 30 - 60 nm in real space. This tendency suggests that a certain phase exists in this scale, whose scattering length density is different from that of the phase I and phase II mentioned above.

## 4 Summary

An experimental station dedicated for SAXS measurements in 2000 - 4000 eV has just been arranged at BL27SU, where a wide measurable  $q$ -range of  $0.005 - 0.5 \text{ nm}^{-1}$  (1000 - 10 nm in real space) and a high flux of  $10^{10}$  photons/s/100mA/0.03%B.W. are achieved. ASAXS experiment near sulfur  $K$ -edge was performed in this experimental station, which gives us some clues to the elucidation of inhomogeneities of crosslinking structure in rubber.

## References

- [1] H. B. Stuhrmann, *Q. Rev. Biophys.*, **14**, 433 (1981).
- [2] H. Ohashi *et al.*, *Rev. Sci. Instrum.*, **73**, 1588 (2002).
- [3] M. Handa *et al.*, *J. Phys.: Conf. Ser.*, **247**, 012006 (2010).
- [4] M. Handa *et al.*, *J. Phys.: Conf. Ser.*, in press.
- [5] Y. Tamenori *et al.*, *Rev. Sci. Instrum.*, **73**, 3 (2002).

## Publications

1. M. Handa, Y. Shinohara, H. Kishimoto, Y. Tamenori and Y. Amemiya, *J. Phys.: Conf. Ser.*, **247**, 012006 (2010).
2. M. Handa, Y. Shinohara, H. Kishimoto, Y. Tamenori, N. Yagi and Y. Amemiya, *J. Phys.: Conf. Ser.*, in press.

## Presentations

1. M. Handa *et al.*, XIV International conference on Small-Angle Scattering (2009).
2. 半田昌史 他, 第 23 回日本放射光学会年会・放射光科学合同シンポジウム (2010), 学生発表賞.
3. M. Handa *et al.*, JST ERATO and CREST Joint Symposium (2010), Best Poster Award.
4. 半田昌史 他, 第 24 回日本放射光学会年会・放射光科学合同シンポジウム (2011).

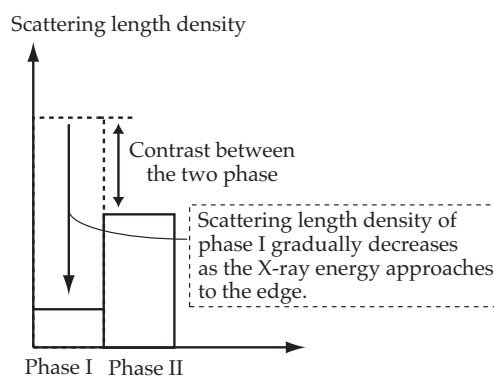


Figure 4: Schematic diagram of the change of the contrast, which is illustrated on the assumption that only phase I contains sulfur atoms.